ECOGRAPHY

Research

Time of emergence of novel climates for North American migratory bird populations

Frank A. La Sorte, Daniel Fink and Alison Johnston

F. A. La Sorte (http://orcid.org/0000-0001-8521-2501) (fal42@cornell.edu), D. Fink (http://orcid.org/0000-0002-8368-1248) and A. Johnston (http://orcid.org/orcid.org/0000-0001-8221-013X), Cornell Laboratory of Ornithology, Cornell Univ., Ithaca, NY, USA. AJ also at: Dept of Zoology, Conservation Science Group, Univ. of Cambridge, Cambridge, UK.

Ecography
42: 1–13, 2019
doi: 10.1111/ecog.04408

Subject Editor: Morgan Tingley
Editor-in-Chief: Miguel Araújo
Accepted 6 February 2019

To better understand the ecological implications of global climate change for species that display geographically and seasonally dynamic life-history strategies, we need to determine where and when novel climates are projected to first emerge. Here, we use a multivariate approach to estimate time of emergence (ToE) of novel climates based on three climate variables (precipitation, minimum and maximum temperature) at a weekly temporal resolution within the Western Hemisphere over a 280-yr period (2021–2300) under a high emissions scenario (RCP8.5). We intersect ToE estimates with weekly estimates of relative abundance for 77 passerine bird species that migrate between temperate breeding grounds in North America and southern tropical and subtropical wintering grounds using observations from the eBird citizen-science database. During the non-breeding season, migrants that winter within the tropics are projected to encounter novel climates during the second half of this century. Migrants that winter in the subtropics are projected to encounter novel climates during the first half of the next century. During the beginning of the breeding season, migrants on their temperate breeding grounds are projected to encounter novel climates during the first half of the next century. During the end of the breeding season, migrants are projected to encounter novel climates during the second half of this century. Thus, novel climates will first emerge ca 40–50 yr earlier during the second half of the breeding season. These results emphasize the large seasonal and spatial variation in the formation of novel climates, and the pronounced challenges migratory birds are likely to encounter during this century, especially on their tropical wintering grounds and during the transition from breeding to migration. When assessing the ecological implications of climate change, our findings emphasize the value of applying a full annual cycle perspective using standardized metrics that promote comparisons across space and time.

Keywords: annual cycle, eBird, global climate change, novel climates, seasonal bird migration, time of emergence

www.ecography.org

Introduction

The ecological implications of global climate change (IPCC 2013) have been documented from a variety of different biological perspectives (Scheffers et al. 2016, Pacifici et al. 2017). When individual species are examined, climate change has been shown to affect species' distributions, phenology, reproductive success and survival (Chen et al. 2011, Johnston et al. 2013, Selwood et al. 2014, Stephens et al. 2016). When estimating the projected implications of climate change for individual species, a common approach to is to determine how climate change projections are defined within species' geographic distributions. This approach typically interprets the absolute magnitude of projected changes in climate, typically temperature, as a measure of ecological significance. One limitation of this approach is that magnitude alone does not provide a consistent measure of ecological significance; i.e. similar magnitudes may generate very different ecological outcomes across regions and seasons. To promote more realistic assessments, it would be valuable to standardize climate change projections under a common baseline that supports comparisons across space and time. One method to accomplish this is to standardize climate change projections by historical year-to-year climatic variation (Williams et al. 2007). The expectation under this approach is that the stronger the deviation from historical variation, the more novel the projected changes in climate and the more significant any resulting ecological disruptions (Williams and Jackson 2007, Fitzpatrick et al. 2018). These disruptions may generate 'ecological surprises' or new ecological domains that lack current analogs (Williams and Jackson 2007, Morse et al. 2014), a process that may be compounded by the influence of other global change drivers (Paine et al. 1998). The associated changes in ecosystem structure and function will have broad ramifications for natural communities that could affect processes such as colonization, extirpation, adaptation and speciation (Bull and Maron 2016, Hulme 2016, Meester et al. 2017).

A common method to summarize standardized climate change projections is to estimate the year when the projection first exceeds some measure of climatic variability, an approach often referred to as time of emergence (ToE) (Hawkins and Sutton 2012). By estimating when climate change is projected to pass a certain threshold of natural variability, ToE simplifies the interpretation of standardized climate change projections by converting probabilities of novel climates to a single estimate of time. ToE therefore identifies a future time period after which natural systems will occur in climates that have no historical analogs at those locations (Williams et al. 2007). How natural systems will be affected by these new associations cannot be readily predicted based on historical associations without applying questionable extrapolations (Fitzpatrick et al. 2018, Qiao et al. 2018). Thus, ToE defines a point in the future where uncertainty crosses a statistical threshold and climate change is likely to generating ecological disruptions whose outcome cannot be accurately predicted (Williams and Jackson 2007).

The most common application of ToE is to examine projected changes in temperature under climate change (Diffenbaugh and Scherer 2011, Mahlstein et al. 2011, 2012a, Hawkins and Sutton 2012, Mora et al. 2013). There are additional examples that consider other climate change factors such as projected changes in precipitation (Giorgi and Bi 2009, Mahlstein et al. 2012b, Douglas 2013, Sui et al. 2014, Nguyen et al. 2018), projected changes in the frequency and intensity of climate extremes (King et al. 2015, Bador et al. 2016, Lee et al. 2016, Tan et al. 2018), projected changes in sea level (Lyu et al. 2014), and projected changes in width of the earth's tropical belt (Quan et al. 2018). A common method for estimating ToE is to identify the year in which the ratio between climate change and historical climatic variability (signal-to-noise ratio) first crosses a predefined threshold, such as one or two (Hawkins and Sutton 2012). A variant of this approach is to identify the year when the signal-to-noise ratio exceeds a predefined threshold across multiple consecutive years (Mora et al. 2013). A common feature of current ToE studies is that ToE is estimated using an annual measure of climate based on one climate variable. Thus, how ToE varies seasonally has not been explored in detail, and how ToE is defined based on a combination of climate variables has not been considered. In addition, ToE has rarely been explored within an ecological context.

The application of a full annual cycle perspective is considered essential in ecological climate change research, especially when examining species that display geographically and seasonally dynamic life-history strategies (Ådahl et al. 2006, Small-Lorenz et al. 2013, Zeigler 2013). A key example and a model research system are migratory birds (Parmesan 2006). These species conduct regular and often broad-scale seasonal movements in response to seasonal variation in resource availability. For bird species that breed in North America and migrate within the Western Hemisphere, a full annual cycle perspective has been used to explore how migratory bird populations are associated with projected changes in temperature and precipitation based on the projected magnitude of change (La Sorte et al. 2017a) and the projected novelty of those changes (La Sorte et al. 2018). Our objective in this study is to advance upon this previous work by translating probabilities of novel climates to estimates of ToE.

Here, we intersect weekly estimates of relative abundance for 77 migratory bird species that breed in North America and migrate within the Western Hemisphere (Supplementary material Appendix 1 Table A1) with weekly estimates of ToE (Fig. 1). We estimate relative abundance for each species using 13 yr of bird observations (2004–2016) from the eBird citizen-science database (Sullivan et al. 2014). We generate weekly estimates of ToE using a multivariate approach (Mahony et al. 2017) based on 60 yr of historical climatic observations (1957–2016) and projected changes in three climate variables (precipitation rate, minimum and maximum temperature) over a 280-yr period (2021–2300). We estimate

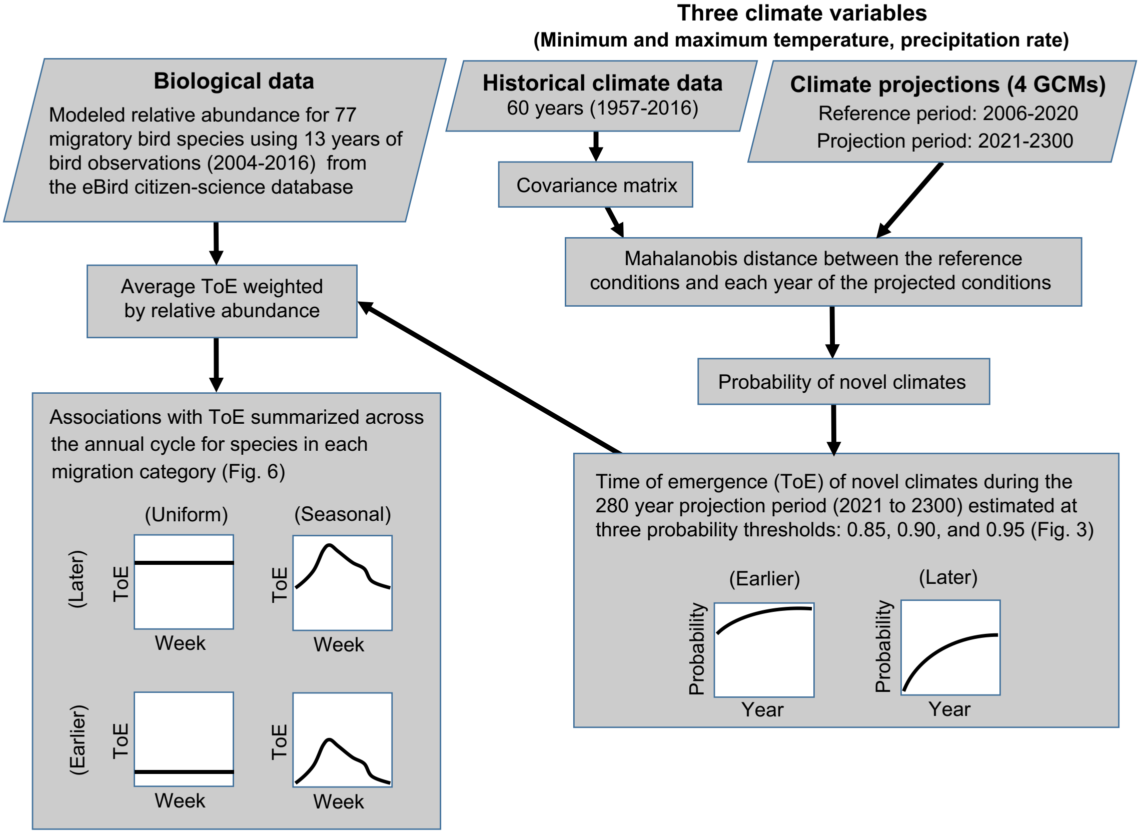

Figure 1. Methodological flow chart illustrating the steps in the time of emergence (ToE) analysis. The analysis was implemented within the Western Hemisphere at a weekly temporal resolution within equal-area hexagon cells (spatial resolution = 49 811 km^2) using four atmosphere-ocean general circulation models (Supplementary material Appendix 3 Table A2) (see Material and methods for additional details).

the probability of novel climates emerging for each week of the 280-yr period. We then use this information to estimate ToE for each week based on the first year a predefined threshold is crossed using the probabilities modeled over the 280-yr period.

Within the Western Hemisphere, climate change projections and year-to-year variation in climate display a variety of spatial and seasonal patterns (La Sorte et al. 2018) that largely determine how ToE estimates will likely be defined for these species. Year-to-year climatic variation is greatest within temperate latitudes, where it displays greater seasonality, and lowest within tropical latitudes, where it displays limited seasonality. Within tropical latitudes where climate change projections are weak (IPCC 2013), the probability of novel climates emerging by the end of this century is projected to be high across all seasons of the year (La Sorte et al. 2018). Within temperate latitudes where climate change projections are stronger (IPCC 2013), the probability of novel climates emerging by the end of this century is projected to be highest during the late summer and early autumn when warming projections are strong and year-to-year variation is at its lowest (La Sorte et al. 2018). Therefore, we expect the 77 migratory bird species considered in this study to display three associations with ToE: 1) earlier ToE during the non-breeding season for species that winter further south within the tropics; 2) later ToE during the breeding season when species are on their temperate breeding grounds; and 3) limited variation in ToE when species occur on their tropical non-breeding grounds, and more substantial variation in ToE when species occur on their temperate breeding grounds. By testing these predictions, our goal is to advance our understanding on how the ecological implications of climate change are likely to develop across space and time for migratory bird species based on their current distributions. Our broader aim is to provide a more robust ecological context for identifying when and where novel climates are likely to significantly affect natural systems.

Material and methods

We located our study area within terrestrial regions of the Western Hemisphere (longitude 30–170°W, latitude 60–84°N; Fig. 2). From a total of 234 bird species available for analysis (Supplementary material Appendix 1 Table A1), we selected migratory passerine species for analysis that migrate between temperate breeding grounds in North America and

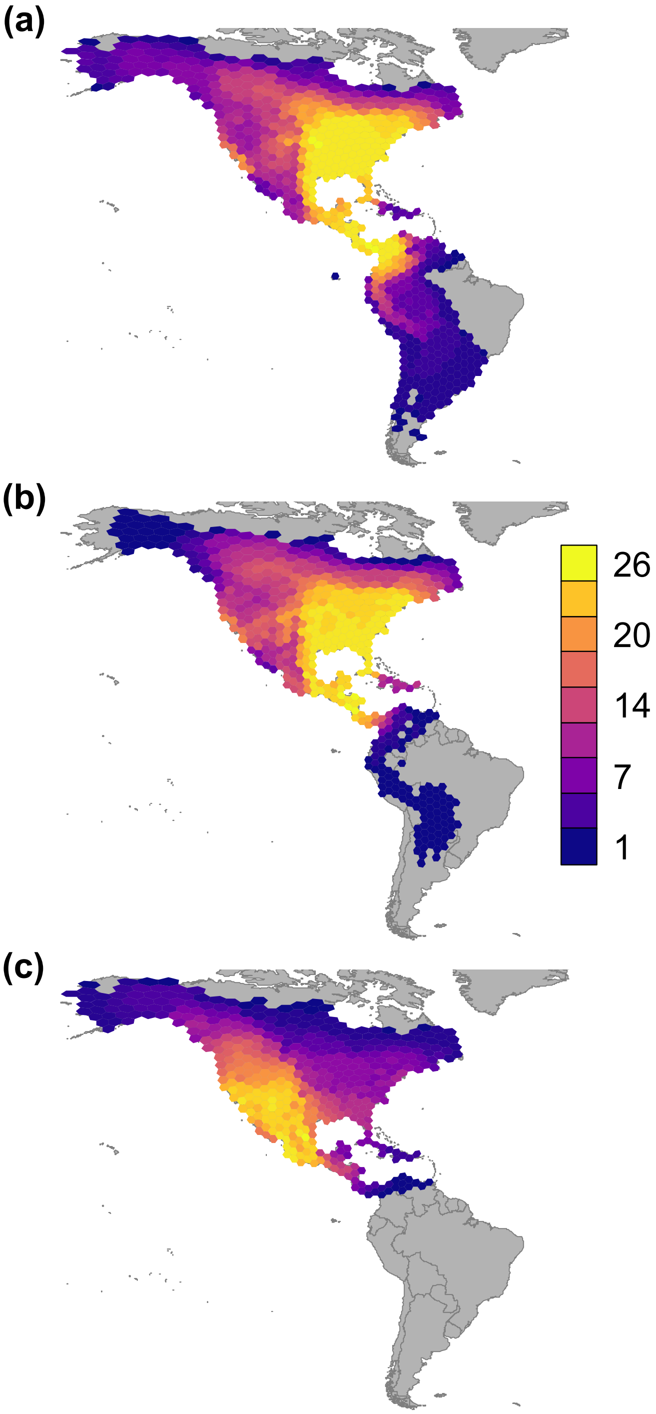

Figure 2. Species richness summarized across the annual cycle for 77 North American migratory bird species (Supplementary material Appendix 1 Table A1) organized into three categories based on the latitude of the center of species' non-breeding distributions: (a) −23.1 to 14.3°, (b) 14.3–18.9° and (c) 18.9–23.3°. Species richness was summarized within equal-area hexagon cells (spatial resolution = 49 811 km^2) of an icosahedral discrete global grid system (see Material and methods for details).

tropical and subtropical wintering grounds using the procedure described in La Sorte et al. (2018). Specifically, we used range map based estimates of geographic centers of occurrence (described below) to identify species whose breeding ranges were centered north of 24°N latitude, whose non-breeding ranges were centered south of 24°N latitude and whose non-breeding maximum latitude occurred south of 34°N latitude. We selected 24°N latitude because it roughly delineates the northern boundary of the tropics, and we selected 34°N latitude because it roughly delineates the northern boundary of the subtropics. This procedure resulted in a total of 92 species for analysis (Supplementary material Appendix 1 Table A1). From these, we removed 15 species whose weekly estimates of relative abundance (described below) did not encompass all 52 weeks of the annual cycle, resulting in 77 species for analysis (Supplementary material Appendix 1 Table A1). We classified the 77 species into three categories based on the latitude of the geographic center of their non-breeding distributions (range = 23.1°S to 23.3°N latitude). Specifically, we divided the 77 species into three groups of roughly equal size based on the 0.33 and 0.67 quantiles of the distribution of the non-breeding season latitudes (14.3°N and 18.9°N latitude, respectively). We chose this approach because, unlike the breeding distributions which were all situated within temperate latitudes, the non-breeding distributions occurred across a broader range of tropical and sub-tropical latitudes.

We identified geographic centers of occurrence for each species' breeding and non-breeding distribution using range maps from NatureServe (Ridgely et al. 2007). The static representation of extent of occurrence provided by the range maps addressed the requirements for our species selection process and non-breeding season classification. We first converted range map polygons to equal-area hexagons having a cell size of 49 811 km^2 and radius of roughly 126 km, generated using a icosahedral discrete global grid system based on a Fuller icosahedral projection using an aperture 4 hexagon partition method (Sahr et al. 2003, Sahr 2011). We selected equal-area hexagon cells for our analysis because they minimize edge effects, the size and shape of the cells are consistent across space, including latitude, and the spatial resolution encompasses the fine and much of the coarse spatial data used in our analysis (details provided below). We calculated geographic centroids by averaging the geographic locations of the hexagon cell-centers occurring within each species' non-breeding and breeding distributions. We only considered hexagon cells that contained greater than 10% terrestrial (non-marine) surface area in these calculations.

Species abundance data preparation and analysis

We estimated species' relative abundance at a weekly temporal resolution and 8.4 × 8.4 km spatial resolution for each of the 77 species within the Western Hemisphere using spatiotemporal exploratory models (STEM) (Fink et al. 2010, 2013, Johnston et al. 2015) and bird observations from the eBird citizen-science database (Sullivan et al. 2014) acquired from the 2016 eBird Reference Dataset. Relative abundance is defined as a relative measure that is only valid for a given species and season, and is not an absolute measure that can be compared across species or seasons. The eBird data included species counts from complete checklists that contained effort information and were collected under the 'traveling count' and 'stationary count' protocols from 1 January 2004 to 31 December 2016. This procedure resulted in a dataset consisting of over 14 million checklists collected at over 1.7 million unique locations (Supplementary material Appendix 2 for additional details). To support our analysis, we aggregated weekly estimates of relative abundance spatially for each of the 77 species by averaging relative abundance values within the equal-area hexagon cells described above.

To support our seasonal interpretation of ToE for each species, we used the average relative abundance estimates within the hexagon cells to generate estimates of migration speed. First, we estimated weekly geographic centers of abundance for each species by calculating the weighted centroid of the hexagon cell centers using species' relative abundance as a weighting factor. We then calculated migration speed for each species using the great-circle (orthodromic) distance between sequentially paired weekly centroids. This approach, which documents the movement of the center of a species' entire population and not the movement of individual migratory birds, provides an objective context to assess when species' populations are stationary, on their breeding or non-breeding grounds, or when populations are in migration in the spring and autumn.

Climate data preparation and analysis

Our climate data consisted of three daily climate variables: average surface precipitation rate ($kg\,m^{-2}\,s^{-1}$), minimum surface temperature at 2 m and maximum surface temperature at 2 m. We selected these three variables because they provide a reliable summary of daily climatic conditions, and the three variables were measured in a consistent fashion across the databases used in this study. We estimated inter-annual variation in the three climate variables using historical climate data from the continuing NCEP/NCAR 40-yr reanalysis project (Kalnay et al. 1996) provided by NOAA/OAR/ESRL PSD (<www.esrl.noaa.gov/psd/>) at a spatial resolution of $2.5 \times 2.5°$. The three variables are identified in the NCEP/NCAR database as prate.sfc.gauss, tmax.2m.gauss and tmin.2m.gauss, respectively. We collected daily estimates for the three climate variables over a 60 yr period (1957–2016; Supplementary material Appendix 4 Fig. A1). We first calculated average weekly values for each of the 60 yr. We then averaged these 52 sets of weekly values within the equal-area hexagon cells for each of the 60 yr using the area of the NCEP/NCAR grid cell that overlapped the hexagon cell as a weighting factor.

We estimated future conditions for the three climate variables using four atmosphere-ocean general circulation models (GCMs; Supplementary material Appendix 3 Table A2) under the Representative Concentration Pathway (RCP) scenario 8.5 from the Coupled Model Intercomparison Project Phase 5 (CMIP5) (IPCC 2013). We acquired data from the World Data Center for Climate (WDCC) during the period 2021–2300 using the Climate and Environmental Retrieval and Archive (CERA) data portal (<http://cera-www.dkrz.de/>). The three climate variables were available at a daily temporal resolution at a variety of horizontal spatial resolutions (0.9–1.875°; Supplementary material Appendix 3 Table A2).

The RCP8.5 scenario is the strongest greenhouse gas forcing scenario, characterized by greenhouse gas emissions and concentrations that increase considerably over this century, leading to a radiative forcing of $8.5\,W\,m^{-2}$ by 2100 (Riahi et al. 2011). RCP8.5 does not include any mitigation targets. RCP8.5 represents the upper bound or worst case scenario where there is no mitigation and demographic, economic and technological drivers follow more extreme trajectories. A recent assessment suggest emissions are currently tracking just above the RCP8.5 scenario (Sanford et al. 2014), and there is evidence that GCM projections under the RCP8.5 scenario have underestimated warming during this century by ca 15% (Brown and Caldeira 2017). Therefore, given current knowledge, we consider RCP8.5 to be a more relevant scenario. However, GCMs contain many sources of uncertainty that may act to enhance or reduce the quality of their projections. For example, there is evidence that the sensitivity of the climate to increasing greenhouse gas emissions is lower than previously estimated (Cox et al. 2018). Conversely, there is evidence that natural feedback processes that are not included in current GCMs may act to enhance global warming (Comyn-Platt et al. 2018).

Our procedure to estimate projected changes in the three climate variables first involved extracting gridded values from each of the four GCMs by day for the years 2021–2300. We defined weekly reference conditions by averaging the three climate variables across days for each week of the year for the years 2006–2020 (15-yr period). We then averaged these weekly values across years to generate 52 weekly reference values for each variable and GCM. We calculated the projected conditions for the years 2021–2300 (280-yr period) by averaging each of the three climate variables by week and year for each GCM. This procedure generated 280 weekly values for each climate variable and GCM. To place the reference and projected conditions within the same spatial configuration for analysis, we averaged the weekly values for the three climate variables within the equal-area hexagon cells where a GCM grid cell was included if the cell center was located inside the hexagon cell.

Time of emergence of novel climates

We generated estimates of ToE using the following procedure (Fig. 1). We calculated the standardized multivariate distance between the reference conditions (2006–2020) and the projected conditions for each hexagon cell, week, GCM and year (2021–2300) using Mahalanobis distance (Mahalanobis 1936) and the covariance matrix of the 60 yr climatic time series (1957–2016). Mahalanobis distance provides a multivariate estimate of the projected departure of future climate conditions from historical inter-annual climate variability for all three climate variables in combination. We converted the squared Mahalanobis distance estimates to probabilities using the Chi-square distribution with three degrees of freedom (Mahony et al. 2017). This procedure resulted in estimates of the probability of novel climates developing within each hexagon cell by week for each GCM and year during the period 2021–2300.

We estimated ToE for each hexagon cell and week using the following procedure (Fig. 3). We applied generalized additive mixed models (GAMMs) (Wood 2017) to the probabilities of novel climates across the 280 yr by hexagon cell and week with GCM included as a random effect. We then extracted the predicted probabilities and associated standard errors for each hexagon cell and week. We then identified the year when the probabilities first exceeded three probability thresholds: 0.85, 0.90 and 0.95 (Fig. 3). This method identified the year after which it is expected that on average the climate will exceed 85, 90 or 95% of the distribution of historical climatic conditions. We considered three thresholds in this analysis to account for the situation where the probabilities did not exceed the threshold during the 280-yr time period considered in the study, an outcome that is likely to be more common at higher probability thresholds (Fig. 3). We repeated this same procedure for the upper and lower 95% confidence bands calculated for each GAMM (Fig. 3). This last step allowed us to estimate the uncertainty in the ToE estimates originating from the four GCMs for each probability threshold.

Time of emergence and migratory birds

We used the following procedure to summarize the weekly associations with ToE for the three probability threshold levels for each of the 77 species of migratory birds (Fig. 1). First, we calculated the weighted average ToE for

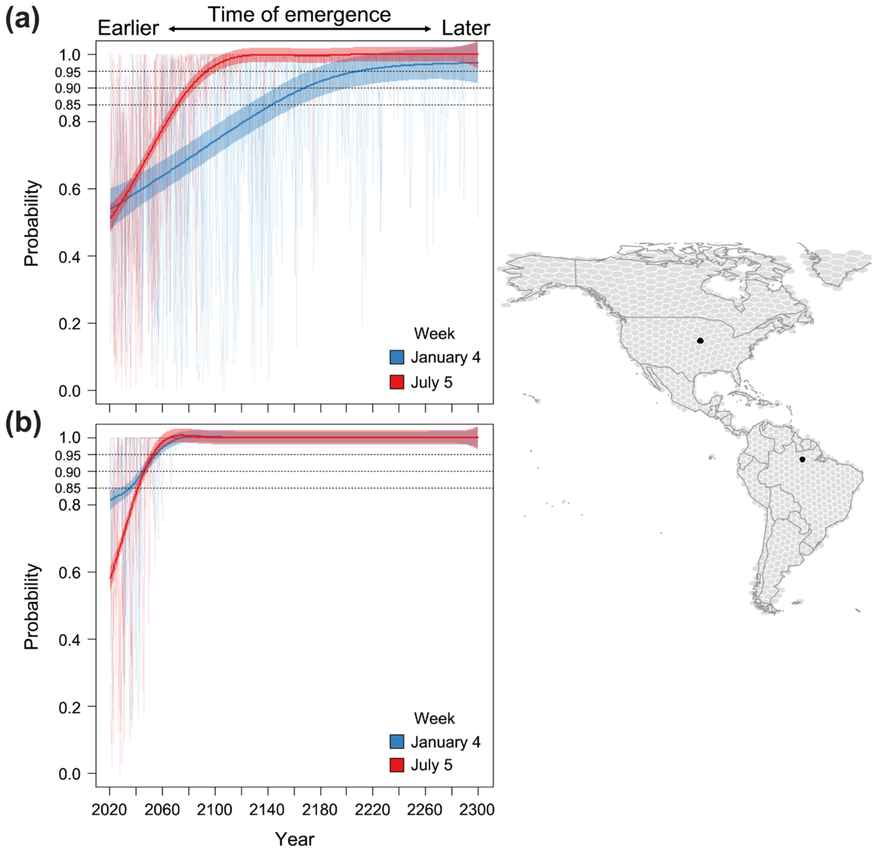

Figure 3. The procedure used to estimate time of emergence (ToE) of novel climates within (a) North America and (b) South America during the week of 4 January (blue) and 5 July (red). The thin colored lines are the probability estimates from the four atmosphere-ocean general circulation models (GCMs; Supplementary material Appendix 3 Table A2). These are the probabilities that the climate will be novel in relation to historical climates during a given week and location. The black dotted lines are the three probability thresholds considered in the analysis. The fitted colored lines and 95% confidence bands are from generalize additive mixed models with GCM included as a random effect (see Material and methods for details). ToE is identified as the year that the fitted GAMM crosses each probability threshold.

each species and week based on the hexagon cells where the species occurred using relative abundance as a weighting factor. This measure describes the average ToE expected to be encountered by a species' entire population during each week. We also calculated the weighted average ToE from the upper and lower 95% confidence bands for each week. This measure described the earliest and latest ToE that a population is expected to encounter during each week among the four GCMs.

We summarized the seasonal patterns in ToE across the year for each of the three groups of species using GAMM with species included as a random effect. The response variables were species' weekly estimates of ToE (2021–2300) and the predictor variables were species as a random effect and week of the year as a smooth spline. We used a cyclic penalized cubic regression spline to smoothly join values estimated for the first week and last week of the year. The use of GAMM in our analysis was valuable because it generated concise graphics that summarized weekly associations with ToE across the year for multiple species simultaneously. We applied this same procedure to ToE based on the upper and lower 95% confidence bands, which we used to generate the confidence band for each species' GAMM fits. These confidence bands allowed us to assess how weekly associations with ToE differed among the three non-breeding season categories. We also summarized the proportion of hexagon cells for each species and week and probability threshold where ToE was estimated to occur after 2300. We summarized how the proportion of missing ToE estimates were defined across the annual cycle for the three non-breeding season categories using GAMM with species included as a random effect and a cyclic penalized cubic regression spline. All analysis was conducted in R, ver. 3.4.3 (R Development Core Team). We used the gamm4 library to implement GAMM (Wood and Scheipl 2017).

Data deposition

Data available from the Dryad Digital Repository: <https://doi.org/10.5061/dryad.4h98fq7> (La Sorte et al. 2019).

Results

Based on our three non-breeding season categories, species that wintered the furthest south occurred at tropical latitudes during the non-breeding season and within temperate regions of eastern North America during the breeding season (Fig. 2a). Species that wintered further north occurred within tropical and subtropical latitudes during the non-breeding season and within temperate regions of eastern North America during the breeding season (Fig. 2b). Species that wintered the furthest north occurred within tropical and subtropical latitudes in western Mexico during the non-breeding season and within temperate regions of western North America during the breeding season (Fig. 2c). The speed of movement of the center of species' populations peaked at similar times during spring (ca 20 April) and autumn migration (ca 11 October) across the three non-breeding season categories, distinguishing periods when species' populations were stationary and when species' populations were in full migration (Fig. 4).

Our ToE projections displayed similar spatial patterns across seasons for the three probability thresholds (Fig. 5, Supplementary material Appendix 4 Fig. A2, A3), suggesting our ToE estimates are not sensitive to the choice of probability threshold. ToE projections were earlier and more consistent across seasons within tropical latitudes. ToE projections were later and more variable across seasons within temperate latitudes, with notably higher variation within the Northern Hemisphere where ToE was earlier during the boreal summer (June–September) and later during the boreal winter (October–May).

Based on the 0.85 probability threshold, almost the entire Western Hemisphere was projected to have novel climates during all seasons by the year 2300 (Fig. 5). The number of locations not projected to have novel climates by the year 2300 increased slightly at the middle probability threshold (0.90), and these locations were concentrated within the mid-latitudes of the Northern Hemisphere during the period from January to February (Supplementary material Appendix 4 Fig. A2). The number of locations not projected to have novel climates by the year 2300 increased dramatically at the highest probability threshold (0.95) and these locations were concentrated within the mid-latitudes of the Northern Hemisphere during the period from December to April

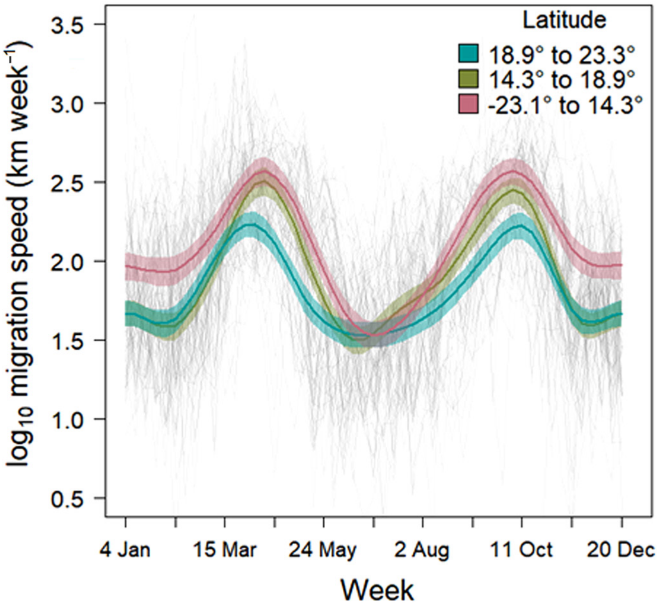

Figure 4. Population-level migration speed summarized by week across the annual cycle for 77 migratory bird species (Supplementary material Appendix 1 Table A1) organized into three categories based on the latitude of the center of species' non-breeding distributions (Fig. 2). The fitted lines and 95% confidence bands are generalize additive mixed models with species included as a random effect.

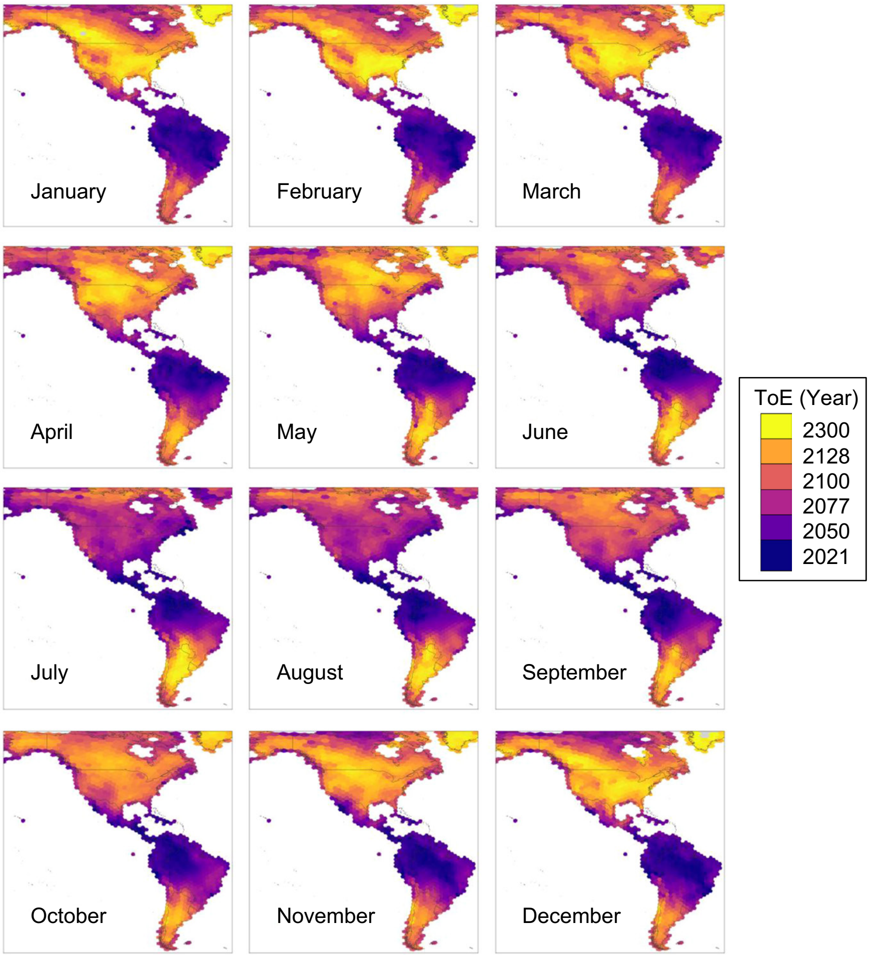

Figure 5. Time of emergence (ToE) summarized monthly at the 0.85 probability threshold level within equal-area hexagon cells (spatial resolution = 49 811 km^2) of an icosahedral discrete global grid system (see Material and methods for details). ToE projections were made during the period from 2012 to 2300. Gray hexagon cells indicate missing ToE values (> 2300).

(Supplementary material Appendix 4 Fig. A3). In total, locations with ToE projections after the year 2300 only occurred within temperate regions during the boreal winter, the time of year when migrants are further south on their non-breeding grounds.

When we intersected the weekly estimates of relative abundance for the 77 migratory bird species with the weekly ToE projections, species' seasonal associations with ToE were generally similar across the three probability thresholds (Fig. 6a, c, e). When examined across seasons (Fig. 4), species' associations with ToE generally differed from one season to the next, and there were distinct differences in ToE among species in the three non-breeding season categories (Fig. 6a, c, e). During the non-breeding season, species that wintered further south (Fig. 2a) were associated with the earliest ToE projections on average (ca 2060–2080; Fig. 6a, c, e), and species that wintered further north (Fig. 2c) were associated with the latest ToE projections on average (ca 2100–2120; Fig. 6a, c, e). Outside the non-breeding season (Fig. 4), similar associations with ToE were documented for all species during spring and autumn migration and during the breeding season (Fig. 6a, c, e). As species moved north to similar latitudes in the spring, all species were associated with later ToE projections (ca 2100–2140), especially species that wintered further south (Fig. 6a, c, e). ToE associations then steadily declined to earlier ToE projections during the breeding season for all species (ca 2070–2090; Fig. 6a, c, e). ToE associations then rose slightly at the end of the breeding season and the beginning of autumn migration before returning to the original non-breeding season levels (Fig. 6a, c, e). In sum, species that winter further south (Fig. 2a) are projected to first encounter novel climates during the non-breeding season (Fig. 4, 6a, c, e), and species that winter further north (Fig. 2c) are projected to first encounter novel climates at the end of the breeding season and the beginning of autumn migration (Fig. 4, 6a, c, e).

The proportion of hexagon cells with missing ToE projections (> 2300) for species in the three non-breeding season categories differed across the three probability thresholds (Fig. 6b, d, f). Missing ToE projections were largely absent at the lowest probability threshold (0.85; Fig. 6b), increased slightly at the intermediate probability

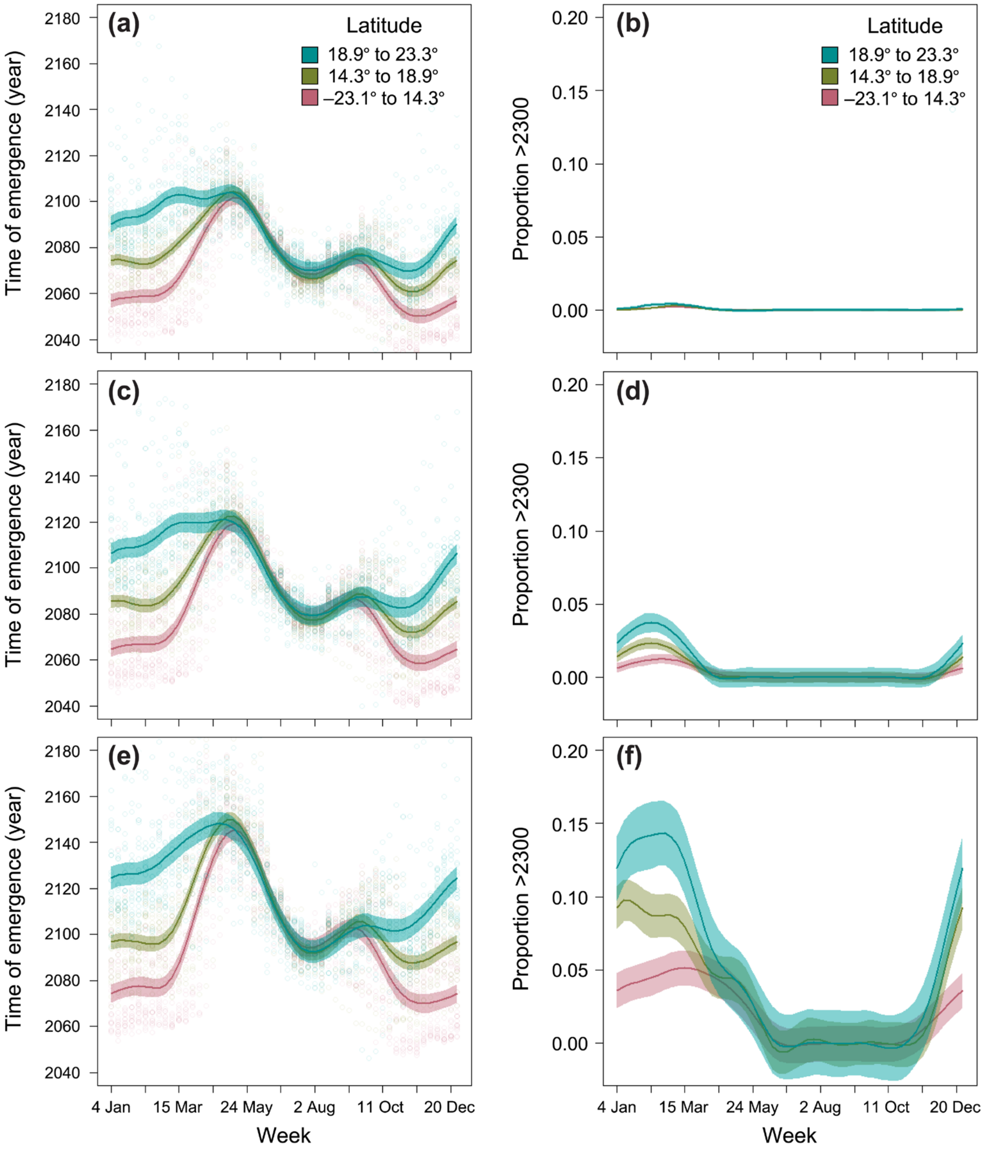

Figure 6. Left column: weekly associations with time of emergence (ToE) during the period from 2021 to 2300 for 77 North American migratory bird species organized into three categories based on the latitude of the center of species' non-breeding distributions (Fig. 2, Supplementary material Appendix 1 Table A1). Right column: the proportion of species' weekly distributions with missing ToE values (> 2300). ToE was estimated at three probability threshold levels: 0.85 (top row), 0.90 (middle row) and 0.95 (bottom row). ToE estimates were made across four atmosphere-ocean general circulation models (Supplementary material Appendix 3 Table A2). The fitted lines and 95% confidence bands are generalized additive mixed models with species included as a random effect (see Material and methods for details).

threshold (0.90; Fig. 6d), and increased substantially at the highest probability threshold (0.95; Fig. 6f). Missing ToE projections only occurred during the boreal winter, and the proportions were greatest for species that wintered further north (Fig. 2c). Thus, breeding season associations were not affected by missing ToE projections, non-breeding season associations were affected at the highest probability threshold (Fig. 6e), and this was most pronounced for species that breed in western North America (Fig. 2c).

Discussion

Our findings describe a timeline on how associations with novel climates under global climate change are likely to develop across the annual cycle for a collection of North American migratory bird species. For species that winter further south within the tropics, migrants are projected to encounter novel climates during the second half of this century. For species that winter further north within the subtropics, migrants are projected to encounter novel climates during the first half of the next century. On their temperate breeding grounds in North America, projected associations with novel climates converge upon a similar timeline. During the beginning of the breeding season, migrants are projected to encounter novel climates during the first half of the next century. During the end of the breeding season, migrants are projected to encounter novel climates during the second half of this century. The difference in encounter times between the beginning and end of the breeding season represents a separation of roughly 40–50 yr. In total, our findings indicate that species that winter within the tropics will encounter novel climates sooner and these associations will encompass the full length of the non-breeding season. Novel climates will develop sooner on the temperate breeding grounds for all species during a period at the end of the breeding season when species are transitioning from breeding to autumn migration.

These findings advance upon previous work (La Sorte et al. 2018) by describing how ecological disruptions associated with the formation of novel climates (Williams and Jackson 2007) are projected to unfold over the next 280 yr for this collection of migratory birds species. During this century, migratory birds that winter within the tropics are projected to experience ecological disruptions across the full length of their non-breeding season, encompassing the majority of their annual life cycle (La Sorte et al. 2017a). On their temperate breeding grounds in North America, migrants are projected to experience more limited ecological disruption during the transition from spring migration to breeding, and more pronounced ecological disruptions at the end of the breeding season during the transition from breeding to autumn migration. Over the long term for these species, novel climates will become completely established across the full annual cycle by the middle of the next century.

The ToE estimates in this study indicate the phases of the annual cycle when climate change are most likely to result in ecological surprises, novel ecosystems and altered ecosystem structure and function. We do not provide a physiological connection between climate and birds, a relationship that has been explored within the context of climate change primarily at a theoretical level; for example, in regard to the physiological requirements of migration (Klaassen et al. 2012) or the physiological limitations of species' distributions (Methorst et al. 2017). Rather, we identify when changes in climate are most likely to exceed a historically defined climatic threshold, generating novel climates, ecological disruptions and novel ecological domains. For migratory birds, this outcome may interfere with the ability of species to acquire the resources (food and habitat) necessary for survival and reproduction. Migratory birds are currently responding to climate change through geographic and phenological adjustments (Shaw 2016, Usui et al. 2017, Howard et al. 2018), which could mitigate some of these consequences. How species are currently responding to climate change, however, is highly variable and difficult to predict (Fei et al. 2017, MacLean and Beissinger 2017). A central factor determining a species' ability to respond is evolutionary potential or phenotypic plasticity (Williams et al. 2008). If these factors are constrained, species may not respond effectively, especially if conditions change rapidly and phenotypic plasticity is limited (Charmantier et al. 2008, Charmantier and Gienapp 2014). There is also the possibility responses are currently lagging behind climate change (La Sorte and Jetz 2012, Ash et al. 2016), generating the potential for species to incur a climatic debt (Devictor et al. 2012, Massimino et al. 2015). Within the context of our findings, determining how species will respond to novel climates contains many uncertainties, especially over the extended time periods considered in this study. This uncertainty is compounded by the effects of other global change processes that are known to affect migratory bird populations; e.g. land-use change (La Sorte et al. 2017a, Zurell et al. 2018) and nighttime light pollution (La Sorte et al. 2017b, Van Doren et al. 2017, Cabrera-Cruz et al. 2018). Nevertheless, our findings do provide a basis to identify the geographic regions and seasons where novel climates will first emerge, and where the initial pressure to respond or adapt will be the most pronounced.

Our approach for estimating novelty involved the application of a multivariate method designed to summarize multiple aspects of climate change in one metric (Mahony et al. 2017). We used this approach to generate local estimates of ToE for each week of the year over a 280-yr period using generalized linear models applied to probabilities of novel climates. Unlike previous methods, our approach did not estimate ToE based on the first occurrence of one event or the first occurrence of a combination of events, but by the occurrence of one unique event detected over a 280-yr period using a modelled summary of central tendency (Fig. 3). Our approach avoids some of the inconsistencies and limitations associated with earlier methods, but it does contain several sources of uncertainty. One is related to the choice of climate variables, which may affect how ToE is defined. By considering multiple climate variables in combination, however, we provide a more comprehensive alternative to traditional approaches that examine individual climate variables in isolation. To improve the quality of our findings, it would be valuable to develop methods that document how the individual components of the joint distribution of climate variables contributes to novelty and ToE estimates.

A second issues is related to the presence of trends in the 60 yr of historical temperature data used in this study to estimate inter-annual climatic variation (Supplementary material Appendix 4 Fig. A1). Identifying and removing monotonic increases in temperature that have occurred in the past as a result of global warming is not a trivial task (Wu et al. 2007, Hawkins and Sutton 2012). Successfully identifying and removing these trends would likely reduce historical inter-annual variation, which would increase novelty probabilities and shift our ToE estimates closer to the present. Our ToE estimates could therefore be more conservative in regions where warming under climate change has historically shown monotonically increasing patterns.

A third source of uncertainty is related to how ToE estimates occur over time relative to the end of the time period under consideration, in this case, the year 2300. The majority of our ToE estimates occurred well before 2300, and when ToE could not be estimated within this time period, these values were not included in our analysis. Our results show that ToE estimates that exceeded 2300 were limited to the northern latitudes, and only occurred during the boreal winter when the species considered in this study were located on their southern non-breeding grounds. In addition, ToE values that exceeded 2300 were encountered primarily by species that wintered further north during the non-breeding season, and only at the highest probability threshold considered in this study. Thus, the quality of our ToE estimates were strongest outside of the non-breeding season for all three probability thresholds, and our ToE estimates were skewed to earlier years during the non-breeding season, but this was only evident at the highest probability threshold.

Another source of uncertainty in our ToE estimates is related to year-to-year variation in our estimates of the probability of novel climates. These probability estimates tended to approach one with declining variance over the 280-yr time period, and in many cases the probability estimates reached an asymptote well before 2300, especially within the tropics (Fig. 3). This behavior supports interpreting ToE estimates within the tropics as highly precise (Supplementary material Appendix 4 Fig. A4). Within temperate regions in North America, our probability estimates tended to display higher variances with poorly defined asymptotes (Supplementary material Appendix 4 Fig. A4). ToE estimates originating from these temperate regions should therefore be interpreted as less precise.

Other sources of uncertainty in our ToE estimates originates from the GCMs. The GCMs used in our analysis tended to generate more variable ToE estimates within the temperate latitudes during the boreal winter (Fig. 3). This variability, however, would not affect our ToE estimates because the species considered in the study are located on their southern non-breeding grounds during this time. Another source of uncertainty originates from differences in projected inter-annual climatic variation among the GCMs (Kharin et al. 2013). Because we modeled central tendency to estimate ToE, differences in year-to-year variation among the GCM projections had little effect on our ToE estimates. Lastly, GCMs contain internal sources of uncertainty acquired during different stages of the modeling process (Knutti et al. 2009). One approach to address this uncertainty is to summarize GCM projections across an ensemble of models, as we did in this study. Considering multiple GCMs, however, creates additional challenges for analysis and interpretation (Knutti et al. 2009). For example, the quality of ensemble based estimates of ToE may not be as accurate as those originating from a single GCM (Hawkins et al. 2014).

In sum, our findings provide a timeline for assessing where and when climate change is likely to significantly affect migratory bird populations. Our results emphasize the large seasonal variation in the formation of novel climates across geographic regions, and the variable challenges migratory birds are likely to encounter during different phases of their annual life cycles. In agreement with previous findings (La Sorte et al. 2018), our results identify the non-breeding grounds, especially those located within the tropics, as an important region for the near-term development of significant ecological disruptions under climate change. Our findings also highlight the pronounced near-term challenges that these species are likely to encounter when adults and juveniles are preparing to leave their temperate breeding grounds to embark on their autumn migration journey. Our findings emphasize the value of applying a full annual cycle perspective in ecological climate change research, and the value of applying a standardized climate change metric that promotes comparisons across space and time. This approach has particular relevance when assessing the ecological implications of climate change for species that display geographically and seasonally dynamic life-history strategies. To advance our understanding on how the ecological implications of novel climates are likely to develop over time, it would valuable to document how novel climates are forming across regions and seasons, and how species are reacting to these changes.

Funding – Funding received from National Science Foundation, Directorate for Biological Sciences, Division of Biological Infrastructure (ABI innovation: DBI-1661329, ABI sustaining: DBI-1356308), National Aeronautics and Space Administration (NNH12ZDA001N-ECOF), The Leon Levy Foundation and The Wolf Creek Charitable Foundation. Computing support from the National Science Foundation (CNS-1059284 and CCF-1522054) and a Microsoft Azure Research Award (CRM: 0518680).

References

Ådahl, E. et al. 2006. From climate change to population change: the need to consider annual life cycles. – Global Change Biol. 12: 1627–1633.

Ash, J. D. et al. 2016. Tracking lags in historical plant species' shifts in relation to regional climate change. – Global Change Biol. 23: 1305–1315.

Bador, M. et al. 2016. Detection of anthropogenic influence on the evolution of record-breaking temperatures over Europe. – Clim. Dyn. 46: 2717–2735.

Brown, P. T. and Caldeira, K. 2017. Greater future global warming inferred from Earth's recent energy budget. – Nature 552: 45.

Bull, J. W. and Maron, M. 2016. How humans drive speciation as well as extinction. – Proc. R. Soc. B 283: 20160600.

Cabrera-Cruz, S. A. et al. 2018. Light pollution is greatest within migration passage areas for nocturnally-migrating birds around the world. – Sci. Rep. 8: 3261.

Charmantier, A. and Gienapp, P. 2014. Climate change and timing of avian breeding and migration: evolutionary versus plastic changes. – Evol. Appl. 7: 15–28.

Charmantier, A. et al. 2008. Adaptive phenotypic plasticity in response to climate change in a wild bird population. – Science 320: 800–803.

Chen, I. C. et al. 2011. Rapid range shifts of species associated with high levels of climate warming. – Science 333: 1024.

Comyn-Platt, E. et al. 2018. Carbon budgets for 1.5 and 2°C targets lowered by natural wetland and permafrost feedbacks. – Nat. Geosci. 11: 568–573.

Cox, P. M. et al. 2018. Emergent constraint on equilibrium climate sensitivity from global temperature variability. – Nature 553: 319–322.

Devictor, V. et al. 2012. Differences in the climatic debts of birds and butterflies at a continental scale. – Nat. Clim. Change 2: 121–124.

Diffenbaugh, N. S. and Scherer, M. 2011. Observational and model evidence of global emergence of permanent, unprecedented heat in the 20th and 21st centuries. – Clim. Change 107: 615–624.

Douglas, M. 2013. When will trends in European mean and heavy daily precipitation emerge? – Environ. Res. Lett. 8: 014004.

Fei, S. et al. 2017. Divergence of species responses to climate change. – Sci. Adv. 3: e1603055.

Fink, D. et al. 2010. Spatiotemporal exploratory models for broad-scale survey data. – Ecol. Appl. 20: 2131–2147.

Fink, D. et al. 2013. Adaptive spatio-temporal exploratory models: hemisphere-wide species distributions from massively crowd-sourced eBird data. – Twenty-Seventh AAAI Conference on Artificial Intelligence (AAAI-13).

Fitzpatrick, M. C. et al. 2018. How will climate novelty influence ecological forecasts? Using the quaternary to assess future reliability. – Global Change Biol. 24: 3575–3586.

Giorgi, F. and Bi, X. 2009. Time of emergence (TOE) of GHG-forced precipitation change hot-spots. – Geophys. Res. Lett. 36: L06709.

Hawkins, E. and Sutton, R. 2012. Time of emergence of climate signals. – Geophys. Res. Lett. 39: L01702.

Hawkins, E. et al. 2014. Uncertainties in the timing of unprecedented climates. – Nature 511: E3.

Howard, C. et al. 2018. Flight range, fuel load and the impact of climate change on the journeys of migrant birds. – Proc. R. Soc. B 285: 20172329.

Hulme, P. E. 2016. Climate change and biological invasions: evidence, expectations and response options. – Biol. Rev. 92: 1297–1313.

IPCC 2013. Climate change 2013: the physical science basis. Contribution of working group I to the fifth assessment report of the intergovernmental panel on climate change. – Cambridge Univ. Press.

Johnston, A. et al. 2013. Observed and predicted effects of climate change on species abundance in protected areas. – Nat. Clim. Change 3: 1055–1061.

Johnston, A. et al. 2015. Abundance models improve spatial and temporal prioritization of conservation resources. – Ecol. Appl. 25: 1749–1756.

Kalnay, E. et al. 1996. The NCEP/NCAR 40-year reanalysis project. – Bull. Am. Meteorol. Soc. 77: 437–471.

Kharin, V. V. et al. 2013. Changes in temperature and precipitation extremes in the CMIP5 ensemble. – Clim. Change 119: 345–357.

King, A. D. et al. 2015. The timing of anthropogenic emergence in simulated climate extremes. – Environ. Res. Lett. 10: 094015.

Klaassen, M. et al. 2012. Ecophysiology of avian migration in the face of current global hazards. – Phil. Trans. R. Soc. B 367: 1719–1732.

Knutti, R. et al. 2009. Challenges in combining projections from multiple climate models. – J. Clim. 23: 2739–2758.

La Sorte, F. A. and Jetz, W. 2012. Tracking of climatic niche boundaries under recent climate change. – J. Anim. Ecol. 81: 914–925.

La Sorte, F. A. et al. 2017a. Global change and the distributional dynamics of migratory bird populations wintering in Central America. – Global Change Biol. 23: 5284–5296.

La Sorte, F. A. et al. 2017b. Seasonal associations with urban light pollution for nocturnally migrating bird populations. – Global Change Biol. 23: 4609–4619.

La Sorte, F. A. et al. 2018. Seasonal associations with novel climates for North American migratory bird populations. – Ecol. Lett. 21: 845–856.

La Sorte, F. A. et al. 2019. Data from: Time of emergence of novel climates for North American migratory bird populations. – Dryad Digital Repository, <https://doi.org/10.5061/dryad.4h98fq7>.

Lee, D. et al. 2016. Time of emergence of anthropogenic warming signals in the northeast Asia assessed from multi-regional climate models. – Asia-Pac. J. Atmos. Sci. 52: 129–137.

Lyu, K. et al. 2014. Time of emergence for regional sea-level change. – Nat. Clim. Change 4: 1006–1010.

MacLean, S. A. and Beissinger, S. R. 2017. Species' traits as predictors of range shifts under contemporary climate change: a review and meta-analysis. – Global Change Biol. 23: 4094–4105.

Mahalanobis, P. C. 1936. On the generalised distance in statistics. – Proc. Natl Inst. Sci. India 2: 49–55.

Mahlstein, I. et al. 2011. Early onset of significant local warming in low latitude countries. – Environ. Res. Lett. 6: 034009.

Mahlstein, I. et al. 2012a. Emerging local warming signals in observational data. – Geophys. Res. Lett. 39: L21711.

Mahlstein, I. et al. 2012b. Perceptible changes in regional precipitation in a future climate. – Geophys. Res. Lett. 39: L05701.

Mahony, C. R. et al. 2017. A closer look at novel climates: new methods and insights at continental to landscape scales. – Global Change Biol. 23: 3934–3955.

Massimino, D. et al. 2015. The geographical range of British birds expands during 15 years of warming. – Bird Study 62: 523–534.

Meester, L. D. et al. 2017. Genetic adaptation as a biological buffer against climate change: potential and limitations. – Integr. Zool. 13: 372–391.

Methorst, J. et al. 2017. A framework integrating physiology, dispersal and land-use to project species ranges under climate change. – J. Avian Biol. 48: 1532–1548.

Mora, C. et al. 2013. The projected timing of climate departure from recent variability. – Nature 502: 183–187.

Morse, N. B. et al. 2014. Novel ecosystems in the Anthropocene: a revision of the novel ecosystem concept for pragmatic applications. – Ecol. Soc. 19: 12.

Nguyen, T.-H. et al. 2018. Time of emergence in regional precipitation changes: an updated assessment using the CMIP5 multi-model ensemble. – Clim. Dyn. 51: 3179–3193.

Pacifici, M. et al. 2017. Species' traits influenced their response to recent climate change. – Nat. Clim. Change 7: 205–208.

Paine, R. T. et al. 1998. Compounded perturbations yield ecological surprises. – Ecosystems 1: 535–545.

Parmesan, C. 2006. Ecological and evolutionary responses to recent climate change. – Annu. Rev. Ecol. Evol. Syst. 37: 637–669.

Qiao, H. et al. 2018. An evaluation of transferability of ecological niche models. – Ecography doi:10.1111/ecog.03986

Quan, X.-W. et al. 2018. On the time of emergence of tropical width change. – J. Clim. 31: 7225–7236.

Riahi, K. et al. 2011. RCP 8.5–a scenario of comparatively high greenhouse gas emissions. – Clim. Change 109: 33–57.

Ridgely, R. S. et al. 2007. Digital distribution maps of the birds of the Western Hemisphere, ver. 3.0. – NatureServe, Arlington, VA.

Sahr, K. 2011. Hexagonal discrete global grid systems for geospatial computing. – Arch. Photogr. Cartogr. Remote Sen. 22: 363–376.

Sahr, K. et al. 2003. Geodesic discrete global grid systems. – Cartogr. Geogr. Infor. Sci. 30: 121–134.

Sanford, T. et al. 2014. The climate policy narrative for a dangerously warming world. – Nat. Clim. Change 4: 164.

Scheffers, B. R. et al. 2016. The broad footprint of climate change from genes to biomes to people. – Science 354: aaf7671.

Selwood, K. E. et al. 2014. The effects of climate change and land-use change on demographic rates and population viability. – Biol. Rev. 90: 837–853.

Shaw, A. K. 2016. Drivers of animal migration and implications in changing environments. – Evol. Ecol. 30: 991–1007.

Small-Lorenz, S. L. et al. 2013. A blind spot in climate change vulnerability assessments. – Nat. Clim. Change 3: 91–93.

Stephens, P. A. et al. 2016. Consistent response of bird populations to climate change on two continents. – Science 352: 84–87.

Sui, Y. et al. 2014. Time of emergence of climate signals over China under the RCP4.5 scenario. – Clim. Change 125: 265–276.

Sullivan, B. L. et al. 2014. The eBird enterprise: an integrated approach to development and application of citizen science. – Biol. Conserv. 169: 31–40.

Tan, X. et al. 2018. Projected timing of perceivable changes in climate extremes for terrestrial and marine ecosystems. – Global Change Biol. 24: 4696–4708.

Usui, T. et al. 2017. Temporal shifts and temperature sensitivity of avian spring migratory phenology: a phylogenetic meta-analysis. – J. Anim. Ecol. 86: 250–261.

Van Doren, B. M. et al. 2017. High-intensity urban light installation dramatically alters nocturnal bird migration. – Proc. Natl Acad. Sci. USA 114: 11175–11180.

Williams, J. W. and Jackson, S. T. 2007. Novel climates, no-analog communities and ecological surprises. – Front. Ecol. Environ. 5: 475–482.

Williams, J. W. et al. 2007. Projected distributions of novel and disappearing climates by 2100 AD. – Proc. Natl Acad. Sci. USA 104: 5738–5742.

Williams, S. E. et al. 2008. Towards an integrated framework for assessing the vulnerability of species to climate change. – PLoS Biol. 6: e325.

Wood, S. N. 2017. Generalized additive models: an introduction with R. – Chapman and Hall/CRC.

Wood, S. N. and Scheipl, F. 2017. gamm4: generalized additive mixed models using mgcv and lme4. – R package ver. 0.2-5, <https://CRAN.R-project.org/package=gamm4>.

Wu, Z. et al. 2007. On the trend, detrending and variability of nonlinear and nonstationary time series. – Proc. Natl Acad. Sci. USA 104: 14889–14894.

Zeigler, S. 2013. Predicting responses to climate change requires all life-history stages. – J. Anim. Ecol. 82: 3–5.

Zurell, D. et al. 2018. Long-distance migratory birds threatened by multiple independent risks from global change. – Nat. Clim. Change 8: 992–996.

Supplementary material (available online as Appendix ecog-04408 at <www.ecography.org/appendix/ecog-04408>). Appendix 1–4.